Magnetic fields and differential rotation on the pre-main sequence

Stephen C. Marsden*, Ian A. Waite† and Bradley D. Carter†

*Anglo-Australian Observatory, PO Box 296, Epping NSW 1710, Australia
†Faculty of Sciences, University of Southern Queensland, Toowoomba, 4350, Australia

Abstract. Maps of magnetic field topologies of rapidly rotating stars obtained over the last decade or so have provided unique insight into the operation of stellar dynamos. However, for solar-type stars many of the targets imaged to date have been lower-mass zero-age main sequence stars. We present magnetic maps and differential rotation measurements of two-higher mass pre-main sequence stars HD 106506 ($\sim$10 Myrs) and HD 141943 ($\sim$15 Myrs). These stars should evolve into mid/late F-stars with predicted high differential rotation and little magnetic activity. We investigate what effect the extended convection zones of these pre-main sequence stars has on their differential rotation and magnetic topologies.

Keywords: stars:individual:HD 106506 — stars:individual:HD 141943 — stars:magnetic fields — stars:starspots
PACS: 95.75.Fg, 95.75.Hi, 97.10.Ld, 97.10.Qh

INTRODUCTION

Main-sequence stars more massive than $\sim$1.3 $M_\odot$ are thought to have no (or extremely thin) outer convection zones and as such should not generate magnetic fields through a solar-like dynamo. Thus these stars are not very magnetically active. However, during the pre-main sequence phase of their evolution these stars were much cooler with significantly larger radii and are believed to have had significant outer convection zones. Thus these stars may in fact have contained a solar-like dynamo in their youth. In this paper we determine the global magnetic topology (and differential rotation, a key component of the dynamo) of two pre-main sequence stars with masses above 1.3 $M_\odot$, HD 106506 and HD 141943, and compare them to that seen on lower mass stars. The stellar parameters for the two stars are given in Table 1.

OBSERVATIONS AND ANALYSIS

Both stars were observed over an 11 night period in March 2007 using the 3.9-m Anglo-Australian Telescope with the SEMPOL polarimeter in conjunction with the UCLES high-resolution echelle spectrograph [4]. The observations were taken in circularly polarised light (Stokes V).

The technique of Least-Squares Deconvolution, LSD [5], was used to combine the signal in each of several thousand photospheric lines in the echelle spectra into a single high signal-to-noise LSD profile for each observation. The average signal-to-noise values were $\sim$1,000 and $\sim$5,000 for the Stokes I and V LSD profiles respectively.

CP1094, *Cool Stars, Stellar Systems and the Sun: 15th Cambridge Workshop,* edited by E. Stempels

TABLE 1. Stellar parameters of HD 106506 and HD 141943. CZD is the Convection Zone Depth as a fraction of the stellar radius. The Ages, Masses, Convection Zone Depths, and Radii are from pre-main sequence models [9].

Star Name	T_{eff} (K)	Age (Myr)	Mass ($M_\odot$)	Radius ($R_\odot$)	CZD (R_{STAR})	Rotational period (d)	vsini (km/s)
HD 106506	~5900	~10	~1.6	~2.2	~0.18	1.39	80.0
HD 141943	~5800	~15	~1.4	~1.8	~0.16	2.174	35.0

Doppler imaging using the code of [2] was used to recreate photospheric brightness maps of both stars from the Stokes *I* LSD profiles. For the Stokes *V* data, Zeeman Doppler imaging using the spherical harmonic decomposition code of [3] was used to recreate the global magnetic field maps. The resultant maps are shown in Figures 1 and 2.

RESULTS AND DISCUSSION

HD 106506

This star is the slightly younger and more massive of the two stars observed and its brightness image (see Figure 1, where spot occupancy is the spot fraction contained in each grid point mapped on the stellar image) shows that it has a large polar spot and some lower-latitude features. The radial field shows no latitude dependence with both positive and negative field at all latitudes. The azimuthal field, in contrast, is dominated by one polarity and shows a ring of positive field around the pole. Such patterns are similar to that seen on less-massive solar-type stars [4, 6] (although the azimuthal field is usually not as dominated by one polarity as we see here) and could indicate that a similar dynamo mechanism is in operation in HD 106506 as lower-mass stars.

HD 141943

For HD 141943 (see Figure 2) we see a similar global magnetic topology to that of HD 106506 with no latitude dependence of the radial magnetic field and the azimuthal magnetic field being dominated by one polarity (the opposite polarity to HD 106506). This would again lend evidence to a similar dynamo operating in HD 141943 and lower-mass stars. The radial magnetic field of HD 141943 appears to be more complex than HD 106506, but this is most likely due to the lower quality of the Stokes *V* profiles for HD 106506. The brightness topology of HD 141943 is somewhat different to that shown by HD 106506 with a very small polar spot and significant amounts of lower-latitude features. Why is it different to that shown by HD 106506 when the relative depth of the convection zones of the stars are similar? Perhaps it is the absolute depth of the convection zone that matters or could the spot pattern of HD 141943 be due to its slower rotation (see Table 1)?

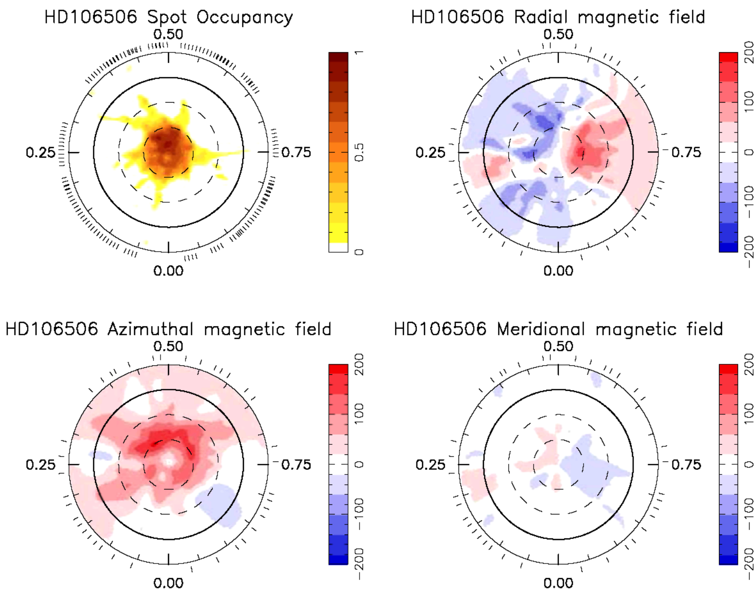

FIGURE 1. Maximum entropy brightness and magnetic images for HD 106506. The images are flattened polar projections extending down to -30° latitude. The bold circles represent the equator and the radial ticks outside each image indicate the phases at which the star was observed. The scale for the magnetic field is in Gauss.

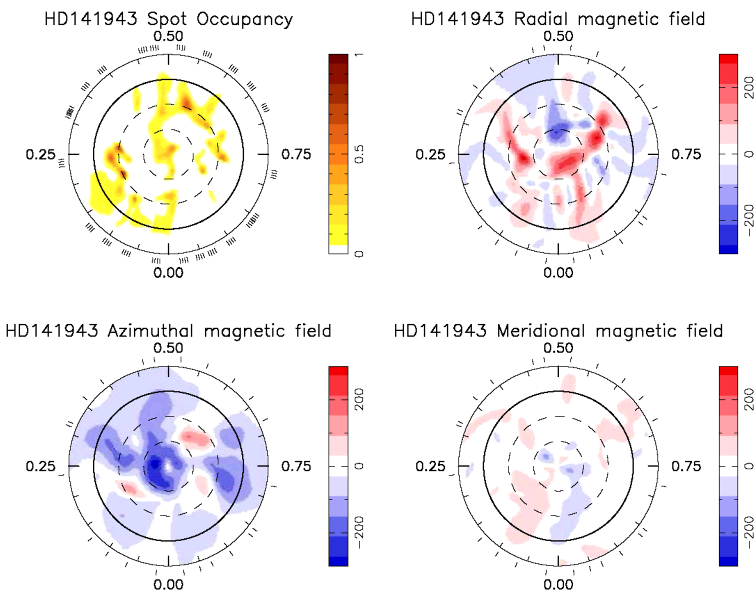

FIGURE 2. Maximum entropy brightness and magnetic images for HD 141943. The images are as described in Figure 1. Note the changed scale on the magnetic images.

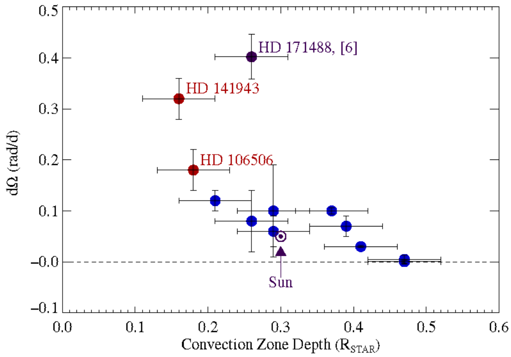

FIGURE 3. Differential rotation (dΩ) versus convection zone depth (as a function of stellar radius). The convection zone depth has been determined from [9] with an assumed error of ± 0.05 R_{STAR}. Blue dots show data from [1]. For stars with multiple measurements an average value was used.

Differential Rotation

By incorporating a differential rotation law into the imaging process it is possible to measure the surface differential of a star. We use a simplified solar-like law:

$$\Omega(l) = \Omega_{eq} - d\Omega sin^2 l(\text{rad/d}), \tag{1}$$

where $\Omega(l)$ is the rotation rate at latitude l, Ω_{eq} is the equatorial rotation rate, and $d\Omega$ is the shear between the equator and poles. By treating Ω_{eq} & $d\Omega$ as free parameters we can use the χ^2-minimisation technique [7] to determine the differential rotation. The level of differential rotation for HD 106506 (from brightness features) and HD 141943 (from magnetic features) is shown in Figure 3.

It appears that differential rotation ($d\Omega$) increases with decreasing convective zone depth until around $0.2R_{STAR}$ where a “jump” in the differential rotation appears to occur. Is this due to a thinning of the stellar convection zone or do other factors play a role?

The high level of differential rotation shown by our targets is supported by the high levels shown on a number of F-stars observed by [8] using line profile analysis.

REFERENCES

1. J. R. Barnes, A. Collier Cameron, J.-F. Donati, D. J. James, S. C. Marsden, and P. Petit, *MNRAS* **357**, L1–L5 (2005)
2. S. F. Brown, J.-F. Donati, D. E. Rees, and M. Semel, *A&A* **250**, 463–474 (1991)
3. J.-F. Donati, *Lect. Not. Phys.* **573**, 207–231 (2001)
4. J.-F. Donati, et al., *MNRAS* **345**, 1145–1186 (2003)
5. J.-F. Donati, M. Semel, B. D. Carter, D. E. Rees, and A. C. Cameron, *MNRAS* **291**, 658–682 (1997)
6. S. C. Marsden, J.-F. Donati, M. Semel, P. Petit, and B. D. Carter, *MNRAS* **370**, 468–476 (2006)
7. P. Petit, J.-F. Donati, and A. Collier Cameron, *MNRAS* **334**, 374–382 (2002)
8. A. Reiners, *A&A* **446**, 267–277 (2006)
9. L. Siess, E. Dufour., and M. Forestini, *A&A* **358**, 593–599 (2000)